Neuron 51, 291–302, August 3, 2006 ©2006 Elsevier Inc. DOI 10.1016/j.neuron.2006.06.029

The Claudin Superfamily Protein NSY-4 Biases Lateral Signaling to Generate Left-Right Asymmetry in *C. elegans* Olfactory Neurons

Miri K. VanHoven,[1] Sarah L. Bauer Huang,[1,2] Stephanie D. Albin,[1] and Cornelia I. Bargmann[1,2,*]
[1] Department of Anatomy and
Department of Biochemistry and Biophysics
The University of California, San Francisco
San Francisco, California 94143
[2] HHMI and
Laboratory of Neural Circuits and Behavior
The Rockefeller University
1230 York Avenue
New York, New York 10025

Summary

Early in *C. elegans* development, signaling between bilaterally symmetric AWC olfactory neurons causes them to express different odorant receptor genes. AWC left-right asymmetry is stochastic: in each animal, either the left or the right neuron randomly becomes AWC^{ON}, and the other neuron becomes AWC^{OFF}. Here we show that the *nsy-4* gene coordinates the lateral signaling that diversifies AWC^{ON} and AWC^{OFF} neurons. *nsy-4* mutants generate 2 AWC^{OFF} neurons, as expected if communication between the AWC neurons is lost, whereas overexpression of *nsy-4* results in 2 AWC^{ON} neurons. *nsy-4* encodes a transmembrane protein related to the γ subunits of voltage-activated calcium channels and the claudin superfamily; it interacts genetically with calcium channels and antagonizes a calcium-to-MAP kinase cascade in the neuron that becomes AWC^{ON}. Genetic mosaic analysis indicates that *nsy-4* functions both cell-autonomously and nonautonomously in signaling between AWC neurons, providing evidence for lateral signaling and feedback that coordinate asymmetric receptor choice.

Introduction

Cell specification often begins with noisy or indeterminate information, but ends in precise, reliable outcomes. Individual olfactory neurons have restricted patterns of receptor expression that define their sensory properties, yet paradoxically in both mammals and *C. elegans* the exact patterns of receptor expression vary from animal to animal and cannot be predicted in advance. In the mammalian olfactory system, a stochastic process causes each olfactory neuron to express only one of the 1000 possible odorant receptor genes (Chess et al., 1994; Lewcock and Reed, 2004; Malnic et al., 1999; Serizawa et al., 2000, 2003). In the nematode *C. elegans*, a stochastic process distinguishes odorant receptor expression in the left and right AWC olfactory neurons (Troemel et al., 1999).

Most of the *C. elegans* nervous system is bilaterally symmetrical, but the left and right AWC olfactory neurons differ in their olfactory properties and in their expression of the G protein-coupled odorant receptor gene *str-2*. *str-2::GFP* reporter genes are expressed either in the left or right AWC neuron in each animal, but never in both (Figure 1A) (Troemel et al., 1999). The *str-2*-expressing neuron, which is called AWC^{ON}, detects the attractive odor 2-butanone, and the *str-2* nonexpressing neuron, which is called AWC^{OFF}, detects the odor 2,3-pentanedione. The left-right asymmetry between AWC neurons enhances odor discrimination as well as odor detection (Wes and Bargmann, 2001).

Bilateral asymmetry has been observed in other *C. elegans* neurons, including other sensory neurons. However, the stochastic nature of AWC asymmetry sets it apart from the reproducible left-right asymmetry in other cases. For example, the left and right ASE taste neurons preferentially sense different ions because of different patterns of gene expression (Pierce-Shimomura et al., 2001). ASE asymmetry is defined through invariant cell lineages that lead to ASEL and ASER and executed by microRNAs and networks of transcription factors (Chang et al., 2003, 2004; Hobert et al., 1999; Johnston and Hobert, 2003, 2005; Johnston et al., 2005; Koga and Ohshima, 2004; Lanjuin et al., 2003; Pierce-Shimomura et al., 2001; Yu et al., 1997). The olfactory and taste systems use different genetic strategies to generate asymmetry: the genes that define ASEL and ASER do not affect AWC asymmetry, and conversely the genes that regulate AWC asymmetry do not affect ASE.

The decision to express *str-2* is made coordinately between the 2 AWC neurons. When the precursor to 1 AWC neuron is killed during embryogenesis, the surviving neuron always becomes AWC^{OFF} (Troemel et al., 1999). This result suggests that communication between the 2 AWC neurons is necessary to trigger the AWC^{ON} receptor choice and that AWC^{OFF} may be a default expression pattern for AWC. In mutants in which the AWC axons are misguided or truncated, both AWC neurons become AWC^{OFF}, suggesting that axons have a role in AWC communication. The 2 AWC axons come into contact with each other in the nerve ring and form synapses with each other, providing a possible site of communication (White et al., 1986), but classical synaptic transmission is probably not required for AWC asymmetry (Troemel et al., 1999). Once the decision is made, receptor choice is stable: ablation of 1 AWC neuron after hatching no longer affects the other AWC (Troemel et al., 1999).

Stochastic decisions in development are often made by lateral signaling, a process in which groups of equivalent cells interact to generate two or more distinct cell types. Many lateral signaling decisions are controlled by the conserved Delta/Serrate/LAG-2 (DSL) family of transmembrane ligands and the LIN-12/Notch family of transmembrane receptors (Greenwald, 1998; Kimble and Simpson, 1997). Despite its stochastic nature, the molecular pathway for AWC receptor choice, as defined by screens for *neuronal symmetry* (*nsy*) mutants, is entirely distinct from the LIN-12/Notch pathway (Troemel et al., 1999). The unknown initial signal between AWC neurons suppresses a calcium-MAP kinase cascade

*Correspondence: cori@rockefeller.edu

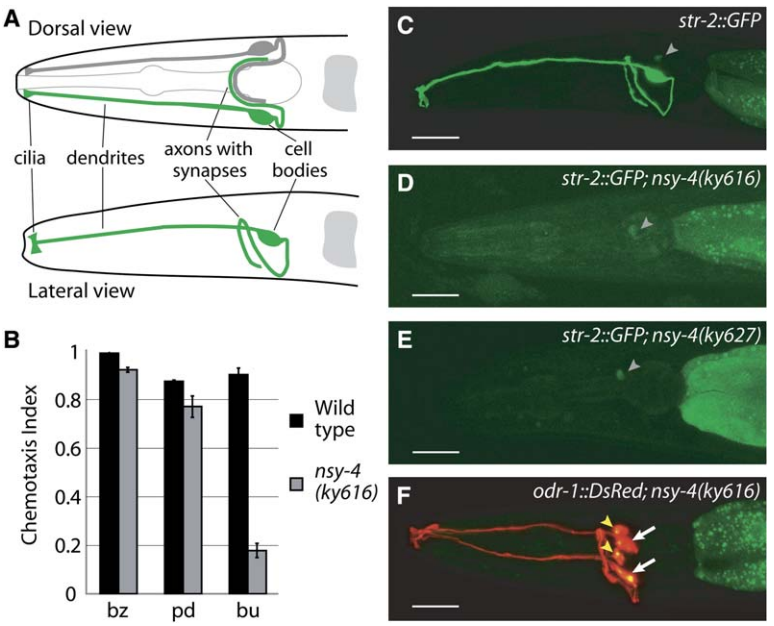

Figure 1. *nsy-4* Mutants Have 2 AWC^{OFF} Neurons

(A) Schematic of wild-type expression of *str-2::GFP* in 1 AWC neuron, AWC^{ON} (green), dorsal and lateral views. The contralateral AWC^{OFF} neuron is diagrammed in gray. (B) Chemotaxis responses of wild-type and *nsy-4(ky616)* animals to the AWC^{OFF}-sensed odorant 2,3-pentanedione (pd), the AWC^{ON}-sensed odorant 2-butanone (bu), and the symmetrically AWC-sensed odorant benzaldehyde (bz). A chemotaxis index of 1 represents 100% of animals approaching the odor; a chemotaxis index of 0 represents random behavior. Error bars indicate SEM. (C–E) *str-2::GFP* expression in (C) wild-type animal, (D) *nsy-4(ky616)* animal, (E) *nsy-4(ky627)* animal. Arrowheads indicate dim *str-2::GFP* expression in the ASI neurons in all strains. (F) *odr-1::RFP* is expressed in both AWC neurons of the *nsy-4(ky616)* animal. Arrows indicate the AWC cell body. AWB neurons also express this marker (yellow arrowheads). All images are projections of confocal stacks. Scale bars, 25 μm. Expression posterior to the AWC cell body is gut autofluorescence.

in 1 AWC neuron that then becomes AWC^{ON} (Chuang and Bargmann, 2005; Sagasti et al., 2001; Tanaka-Hino et al., 2002; Troemel et al., 1999). The calcium-MAP kinase cascade includes the N-type calcium channel α1 and α2/δ subunits UNC-2 and UNC-36, the calcium/calmodulin-dependent kinase CAMKII (UNC-43), the Toll-repeat adaptor protein TIR-1, the MAPKKK NSY-1/ASK1, and the MAPKK SEK-1 (see Figure 5). Loss-of-function mutations in these genes cause both AWC neurons to adopt the AWC^{ON} receptor choice, and gain-of-function mutations cause both neurons to adopt the AWC^{OFF} choice. Genetic mosaic analysis indicates that *unc-43*, *tir-1*, and *nsy-1* are required only in the AWC^{OFF} neuron, downstream of the initial signaling event that diversifies the 2 AWC neurons (Chuang and Bargmann, 2005; Sagasti et al., 2001).

The molecules that mediate the initial signaling between AWC neurons are unknown. The cell ablation studies predict that both AWC neurons should adopt the AWC^{OFF} receptor choice if communication between AWC neurons is lost. Here we describe reduction-of-function mutations in the gene *nsy-4* that cause a 2 AWC^{OFF} phenotype. We find that *nsy-4* encodes a transmembrane protein that participates in communication and feedback between AWC neurons.

Results

nsy-4 Mutants Have 2 AWC^{OFF} Neurons

A screen for mutants in which neither AWC neuron expressed *str-2::*GFP (a 2 AWC^{OFF} phenotype) yielded the two mutations *ky616* and *ky627* (Figure 1 and Table 1). Both alleles were fully recessive and failed to complement each other for the 2 AWC^{OFF} phenotype, defining the new gene *nsy-4* (see Experimental Procedures).

The AWC^{ON} and AWC^{OFF} neurons sense different but overlapping sets of odors (Wes and Bargmann, 2001). The sensory properties of the AWC neurons in *nsy-4* mutants were examined in chemotaxis assays. *nsy-4* animals were proficient in chemotaxis to the odor benzaldehyde, which is sensed by both AWC neurons, and in chemotaxis to 2,3-pentanedione, which is sensed by AWC^{OFF}. However, these animals failed to respond to butanone, which is primarily sensed by AWC^{ON} (Figure 1B). These results suggest that *nsy-4* animals have one or more functional AWC^{OFF} neurons, but no functional AWC^{ON} neurons, and are consistent with the pattern of *str-2* and *odr-1* expression. Thus, *nsy-4* affects both behaviors and gene expression associated with AWC^{ON}.

A 2 AWC^{OFF} phenotype could result from a general disruption of AWC cell fate (as seen in *ceh-36* mutants [Lanjuin et al., 2003]), a defect in axon guidance (as seen in *unc-76*, *sax-5*, *vab-3*, and *sax-3* mutants [Troemel et al., 1999]), or a specific alteration in AWC receptor choice. Generic AWC fate appeared to be specified normally in *nsy-4(ky616)* and *nsy-4(ky627)* mutants, based on expression of the AWC marker *odr-1::dsRed* in 2 AWC neurons (Figure 1F, n ≥ 49 animals). The trajectories of the AWC axons were normal in *nsy-4(ky616)* and *nsy-4(ky627)* (scored with *odr-1::dsRed*; Figure 1F, n ≥ 41 animals), and GFP fusions to the synaptic protein *rab-3* were appropriately distributed in puncta in the AWC axons (data not shown). These results indicate that the 2 AWC^{OFF} phenotype in *nsy-4* mutants is not caused by a general defect in AWC identity or axon guidance.

The initial pattern of AWC receptor choice is established by signaling during embryogenesis but maintained after hatching by a separate pathway including two olfactory guanylate cyclases that are localized to AWC cilia, ODR-1 and DAF-11 (Troemel et al., 1999). This pathway may allow sensory activity to influence receptor expression. Unlike *odr-1* mutants, *nsy-4* mutants did not express *str-2::GFP* in more AWC neurons in early larval stages (Table 1), suggesting that *nsy-4* acts in the initiation, not the maintenance, of AWC receptor choice.

In addition to the 2 AWC^{OFF} phenotype, the *nsy-4(ky627)* allele was weakly dumpy and uncoordinated,

Table 1. *str-2* Expression in Single and Double Mutants

Strain	Percentage of Animals			n
	2 AWC^{ON}	1 AWC^{ON}/1 AWC^{OFF}	2 AWC^{OFF}	
Wild-type	0	100	0	206
nsy-4(ky616)	0	13	87	217
nsy-4(ky627)	0	3	97	141
unc-36(e251)	95	5	0	194
unc-2(lj1)	56	37	7	158
unc-2(e55)	34	47	18	109
unc-43(n1186)	99	1	0	102
nsy-1(ky542)	100	0	0	51
unc-36(e251); nsy-4(ky616)	62	29	9	336*
unc-36(e251); nsy-4(ky627)	78	20	2	138*
unc-2(lj1); nsy-4(ky616)	98	2	0	124*
unc-2(lj1); nsy-4(ky627)	100	0	0	151*
unc-2(e55); nsy-4(ky616)	96	4	0	113
unc-2(e55); nsy-4(ky627)	96	3	1	110
unc-43(n1186); nsy-4(ky616)	98	2	0	117*
nsy-1(ky542); nsy-4(ky616)	100	0	0	51
Wild-type L1/L2	0	0 dim, 100 bright	0	70
odr-1(n1933) L1/L2	0	74 dim, 0 bright	26	68
nsy-4(ky616) L1/L2	0	0 dim, 22 bright	78	93

Asterisks indicate that data is combined from two isolates that exhibited similar proportions of phenotypic classes. Dim *str-2::GFP* expression in L1/L2 animals indicates a defect in maintenance of *str-2::GFP* expression. 100% of adult *odr-1* animals are 2 AWC^{OFF} (Troemel et al., 1999).

grew slowly, and had a small brood size (see Figure S1 in the Supplemental Data available online and data not shown). A dumpy and subviable phenotype has also been reported following RNAi of the *nsy-4* gene (Simmer et al., 2003). These observations suggest that *nsy-4* is an essential gene. Since AWC is not required for viability, normal body size, or fertility (Bargmann et al., 1993), *nsy-4* probably functions in multiple cell types. The AWC cilia were reduced in size in the stronger *nsy-4* mutant, *nsy-4(ky627)* (86% of animals, n = 42), but not in the *nsy-4(ky616)* mutant. AWC receptor choice is normal in many mutants with mildly or severely malformed cilia, including *che-3*, *che-13*, *osm-6*, and *odr-3* (Troemel et al., 1999; E. Troemel and C.I.B., unpublished data). Therefore, the relatively mild cilia malformation of *nsy-4* mutants is unlikely to explain the defect in receptor choice.

nsy-4 Encodes a Four-Transmembrane Domain Protein with Similarity to Claudins and Calcium Channel γ Subunits

The *nsy-4* gene was mapped and cloned by transgenic rescue of the 2 AWC^{OFF} phenotype (see Experimental Procedures). A PCR fragment that contained only the open reading frame for the predicted gene Y38F2AL.1 rescued AWC^{ON} receptor choice in both *nsy-4(ky616)* and *nsy-4(ky627)* mutants (Figure 2D). Sequencing of Y38F2AL.1 revealed missense mutations in both mutant alleles, resulting in a predicted serine to phenylalanine substitution in *ky616* (S43F) and a predicted leucine to phenylalanine substitution in *ky627* (L49F) (Figures 2A and 2B). We conclude that *nsy-4* corresponds to the open reading frame Y38F2AL.1.

nsy-4 encodes a protein with four predicted transmembrane domains and similarity to mammalian γ subunits of voltage-activated calcium channels, the AMPA-regulatory TARP/stargazin proteins, and the claudin multigene family of cell adhesion /tight junction proteins. The amino and carboxy termini of NSY-4 are predicted to be intracellular and the carboxy terminus of NSY-4 ends in a consensus type I PDZ binding motif (Figure 2A).

Direct sequence inspection and PSI-BLAST analysis (Altschul et al., 1997) were used to infer the relationship between *nsy-4* and related proteins. The closest homologs to *nsy-4* are six uncharacterized *C. elegans* genes with similar structures. The closest proteins found in other organisms are the calcium channel γ subunits and the TARPS, followed closely by claudins. All of these proteins have a longer first extracellular domain, a small second extracellular domain, and short conserved sequence motifs including a GLWXXC motif in the first extracellular domain near the residues mutated in the *nsy-4* mutant alleles (Figure 2B) (Arikkath and Campbell, 2003; Chu et al., 2001; Morita et al., 1999). The tetraspanin family of signaling proteins also shares the basic four-transmembrane domain topology of *nsy-4*, but has structural and sequence features that are not present in *nsy-4* (Maecker et al., 1997). The sequence analysis indicates that *nsy-4* belongs to a large, loosely conserved superfamily of claudins and related proteins that has apparently diverged into multigene families independently in *C. elegans* and vertebrates.

nsy-4 cDNAs were isolated and sequenced to establish its gene structure. *nsy-4* can encode four similar proteins of 305 to 316 amino acids that differ in their predicted start sites (optional exon 1, 18 bp) and in alternative splicing of the sixth exon (15 bp). Each of the four cDNAs was able to rescue the 2 AWC^{OFF} phenotype of *nsy-4* mutants (Figure S2). The *nsy-4a* cDNA encoding a protein of 316 amino acids was used for detailed characterization.

RNA interference of Y38F2AL.1 in an *eri-1;lin-15b* mutant background (Duchaine et al., 2006; Kennedy et al., 2004) caused a 2 AWC^{OFF} phenotype (16% 2 AWC^{OFF}, n = 148). Since RNAi decreases mRNA levels, this result suggests that reduction of Y38F2AL.1 function results in a 2 AWC^{OFF} phenotype, the same phenotype caused by the point mutations in *nsy-4*. Overexpression of *nsy-4*

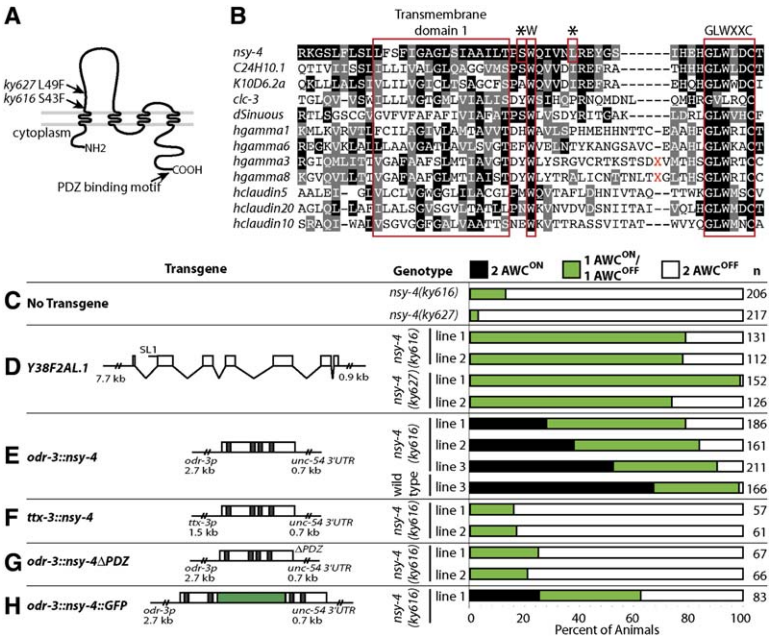

Figure 2. *nsy-4* Encodes a Four-Transmembrane Protein in the Claudin Superfamily

(A) Predicted NSY-4 domain structure. Residues mutated in *ky616* and *ky627* are indicated. The PDZ binding motif is also indicated. (B) Partial alignment of the first transmembrane domain and conserved GLWXXC motif (red boxes) of *nsy-4* with *C. elegans* claudin homologs (C24H10.1, K10D6.2a, *clc-3*), a *Drosophila* claudin (*dSinuous*), human claudins (hclaudin5, hclaudin20, hclaudin10) and human γ subunits and TARPs (hgamma1, hgamma6, hgamma3, hgamma8). Residues mutated in *ky616* and *ky627* are indicated with asterisks. "X" represents stretches of amino acids in hgamma3 and hgamma8 that do not align with the other sequences. (C) *str-2* expression in *nsy-4(ky616)* and *nsy-4(ky627)*. Bars indicate the fraction of animals with each phenotype—2 AWC^{ON}, 2 AWC^{OFF}, and 1 AWC^{ON}/1 AWC^{OFF}. (D) Rescue by genomic *nsy-4* fragment containing Y38F2AL.1, 7.7 kb of upstream sequence, and 0.9 kb of downstream sequence. SL1 *trans*-splice site is indicated. (E) Rescue by *odr-3::nsy-4*, a 2.7 kb *odr-3* promoter driving *nsy-4* cDNAa, in three transgenic lines. Line 3 was also crossed into wild-type animals. Transmembrane domains are shaded black. Lines 1 and 2 were injected at 50 ng/μl. Line 3 was injected at 75 ng/μl. Similar results were obtained with cDNAs b–d (Figure S2). (F) Lack of rescue by *ttx-3::nsy-4*, an ~1.5 kb *ttx-3* promoter driving *nsy-4* cDNAa in AIY (two lines shown are representative of seven tested). (G) Lack of rescue by *odr-3::nsy-4 ΔPDZ*, *odr-3::nsy-4* with the C-terminal PDZ binding motif deleted (two lines shown are representative of six tested). (H) Rescue by *odr-3::nsy-4::GFP*, *odr-3::nsy-4* with GFP coding sequence (green) inserted between transmembrane domains two and three. *odr-3::nsy-4::GFP* was coinjected with *str-2::dsRedII.* n, number of animals scored.

under the AWC-specific *odr-3* promoter in wild-type animals resulted in a 2 AWC^{ON} phenotype opposite to that of the *nsy-4* mutants (Figure 2E). This defect was stronger in wild-type animals than in *nsy-4* mutant animals expressing the same transgene ($p < 0.001$). The results of the RNAi and dosage studies suggest that the two *nsy-4* missense alleles are reduction-of-function alleles.

These results indicate that NSY-4, a protein related to calcium channel subunits, TARPs, and claudins, promotes AWC^{ON} receptor choice. Neither the sequence of *nsy-4* nor rescue experiments placed it firmly in any one branch of the superfamily. Expression of a human claudin in AWC resulted in partial rescue of *nsy-4(ky616)* mutants, expression of a TARP (stargazin/γ2) had weaker effects, and expression of the γ7 calcium channel subunit gave ambiguous results due to dendrite morphology defects (Figure S3). Although there are no one-to-one orthologs in the claudin superfamily between *C. elegans* and vertebrates, the proteins are likely to have conserved functions in adhesion and ion channel regulation (see Discussion).

NSY-4 Can Function in AWC Neurons to Regulate AWC Cell Fate

A transgene with 7.7 kb of sequence upstream of the *nsy-4* start codon and the entire *nsy-4* genomic sequence resulted in efficient rescue of *nsy-4* mutants (Figure 2D). A GFP fusion gene with 7.7 kb of *nsy-4* upstream sequence was expressed beginning at the comma stage of embryogenesis and continuing until the adult (Figure 3A). At the 2-fold stage of embryogenesis, expression was prominent in the excretory cell and in anterior epidermal cells. At the first larval stage, the *nsy-4* reporter transgene was expressed in the excretory cell, in epidermal cells in the head (some or all of hyp 1-6) and tail (some or all of hyp 8-11), and in the P neuro-epidermoblasts, both before and after their ventral migration (Figure 3A). Weak *nsy-4::GFP* expression was detectable in a few neurons.

nsy-4::GFP expression could not be easily scored in AWC, because AWC is immediately adjacent to the excretory cell processes that expressed *nsy-4::GFP* at high levels. Therfore, an extrachromosomal array that included both *nsy-4::GFP* and the punctate AWC marker *odr-3::lin-10::dsRedII* was used to examine *nsy-4::GFP* in AWC. Mosaic animals that spontaneously lost the array from the excretory cell, but retained it in AWC, were identified by loss of excretory *nsy-4::GFP* expression and retention of *lin-10::dsRedII*. AWC is closely related to the excretory cell in the *C. elegans* lineage, so these mosaics were rare. In three appropriate mosaic animals identified at the L1/L2 stage, *nsy-4::GFP* was observed in the AWC cell body (Figures 3B and 3C). Expression was not detectable in AWC in older animals.

The subcellular localization of NSY-4 was determined using a fusion protein in which GFP was inserted between the second and third predicted transmembrane domains of NSY-4. This protein rescued the *nsy-4* mutant phenotype (Figure 2H; several other GFP fusions at other positions in NSY-4 did not rescue). When expressed from the AWC-selective *odr-3* promoter, NSY-4::GFP was membrane associated and excluded from the nucleus. The protein was present throughout the AWC axon, cell body, and dendrite, with highest accumulation at the base of the AWC cilia in adult animals (Figure 3D).

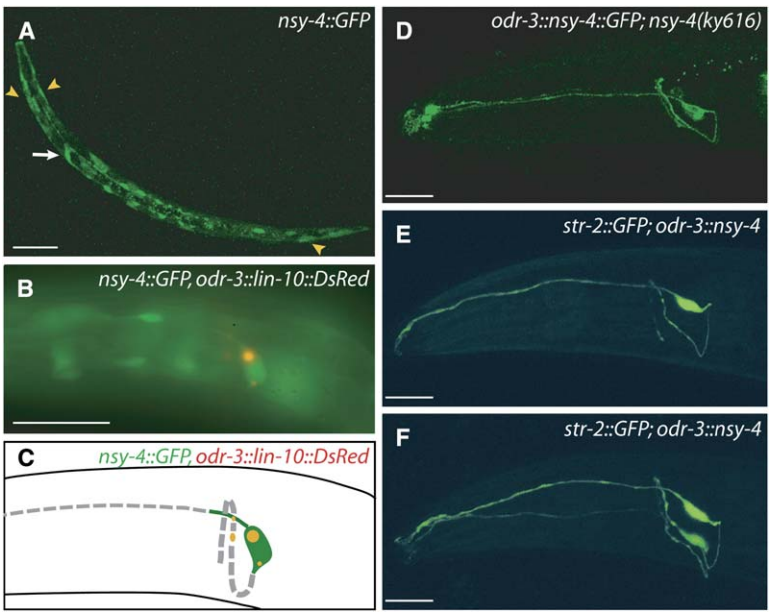

Figure 3. *nsy-4* Is Expressed in AWC Neurons and Epithelial Cells

(A) Confocal projection of L1 animal expressing *nsy-4::GFP* (GFP driven by 7.7 kb of sequence upstream of *nsy-4*). White arrow indicates excretory cell. Yellow arrowheads indicate epidermal cells. (B) Colocalization of *nsy-4::GFP* and *odr-3::lin-10::dsRedII* in late L1/early L2 animal. The *odr-3* promoter drives expression primarily in AWC. LIN-10 accumulates in perinuclear intracellular compartments and in axon puncta. (C) Schematic of (B), indicating colocalization of diffuse GFP and punctate LIN-10::dsRed in AWC. (D) Expression of *odr-3::nsy-4::GFP* in a rescued *nsy-4(ky616)* L4 animal. Note nuclear exclusion of GFP in AWC cell body and expression in dendrite, cilium, and axon. (E and F) *str-2::GFP* in wild-type animals overexpressing *nsy-4* from the *odr-3::nsy-4* transgene (E) wild-type 1-AWC^{ON} phenotype (F) 2-AWC^{ON} phenotype. Scale bars, 25 μm.

To ask whether expression of *nsy-4* in AWC could be sufficient for phenotypic rescue, *nsy-4* cDNAs were expressed under control of the AWC-selective *odr-3* promoter and introduced into *nsy-4* mutants. These transgenes partially rescued *str-2* expression in *nsy-4* animals (Figures 2E and 3E), suggesting that *nsy-4* expression in AWC can drive the AWC^{ON} receptor choice. Mosaic analysis of *str-2::GFP* expression in *odr-3::nsy-4* strains also supported a tight association between expression in AWC and restoration of the AWC^{ON} receptor choice; for example, animals that expressed *nsy-4* in AWB but not AWC were not rescued for *str-2::GFP* expression (n = 4). These results suggest that *nsy-4* can function in AWC to promote the AWC^{ON} receptor choice. The lethality, dumpiness, and sterility of *nsy-4(ky627)* were rescued by the Y38F2AL.1 genomic fragment, but not by *odr-3::nsy-4* transgenes, suggesting that *nsy-4* also functions in other cell types.

Control experiments supported a specific rescuing function of *nsy-4* in AWC for AWC receptor choice. The *ttx-3* promoter drives expression in the interneuron AIY, a primary synaptic partner of AWC. Expression of *nsy-4* under the *ttx-3* promoter failed to rescue *nsy-4* (Figure 2F) and had no effect in a wild-type background (data not shown). An *odr-3::nsy-4* transgene in which the PDZ binding motif was deleted from the *nsy-4* C terminus also failed to rescue *nsy-4*, indicating that an intact *nsy-4* coding region was required for AWC^{ON} receptor choice (Figure 2G).

In addition to their rescue of the 2 AWC^{OFF} phenotype, *odr-3::nsy-4* transgenes caused a 2 AWC^{ON} gain-of-function phenotype, either when injected into a *nsy-4* mutant or when injected into wild-type animals (Figures 2E and 3F). The 2 AWC^{ON} phenotype was more severe when larger amounts of DNA were injected and was weaker in an *nsy-4* mutant than in wild-type animals, indicating that endogenous *nsy-4* cooperates with the *odr-3::nsy-4* transgene to promote the AWC^{ON} phenotype (Figure 2E). The *odr-3* promoter is expressed more strongly in AWC than the endogenous *nsy-4* promoter and stays on throughout the life of the animal, so this gain-of-function phenotype may result from unregulated *nsy-4* expression.

nsy-4 Antagonizes the Calcium Signaling Pathway in AWC

Double mutants between *nsy-4* and other mutations that affect AWC receptor choice were used to ask how *nsy-4* might act to affect AWC development. Null mutations in the type II calcium/calmodulin-dependent kinase *unc-43* result in a strong 2 AWC^{ON} phenotype opposite to that of *nsy-4* mutants (Troemel et al., 1999). *nsy-4 unc-43* double mutants were indistinguishable from *unc-43* single mutants (Table 1). Similarly, *nsy-4 nsy-1* double mutants were indistinguishable from null mutations in *nsy-1*, which encodes the downstream MAPKKK ASK1 (Table 1). These results are consistent with a role for *nsy-4* that is predominantly upstream of or parallel to *unc-43* and *nsy-1.*

The N/P-type calcium channel genes *unc-36* and *unc-2* act upstream of *unc-43* (Troemel et al., 1999). Null mutations in the α2/δ subunit *unc-36* result in a strong 2 AWC^{ON} phenotype, and *nsy-4 unc-36* double mutants resembled *unc-36* single mutants, with a preponderance of 2 AWC^{ON} animals (Table 1). This result suggests that *nsy-4* acts upstream of *unc-36* to inhibit its activity, or parallel to *unc-36* to regulate a common target. However, the 2 AWC^{ON} phenotype was significantly less severe in *nsy-4 unc-36* double mutants than in *unc-36* null mutants, suggesting that *nsy-4* does not act solely by inhibiting *unc-36.*

Animals with null mutations in the calcium channel α1 subunit *unc-2* have a high frequency of 2 AWC^{ON} animals (Mathews et al., 2003; Troemel et al., 1999). Since *unc-2* and *unc-36* are thought to encode subunits of a common channel (Schafer et al., 1996), we expected *nsy-4 unc-2* animals to resemble *unc-2* animals, with a preponderance of 2 AWC^{ON} animals. This expectation

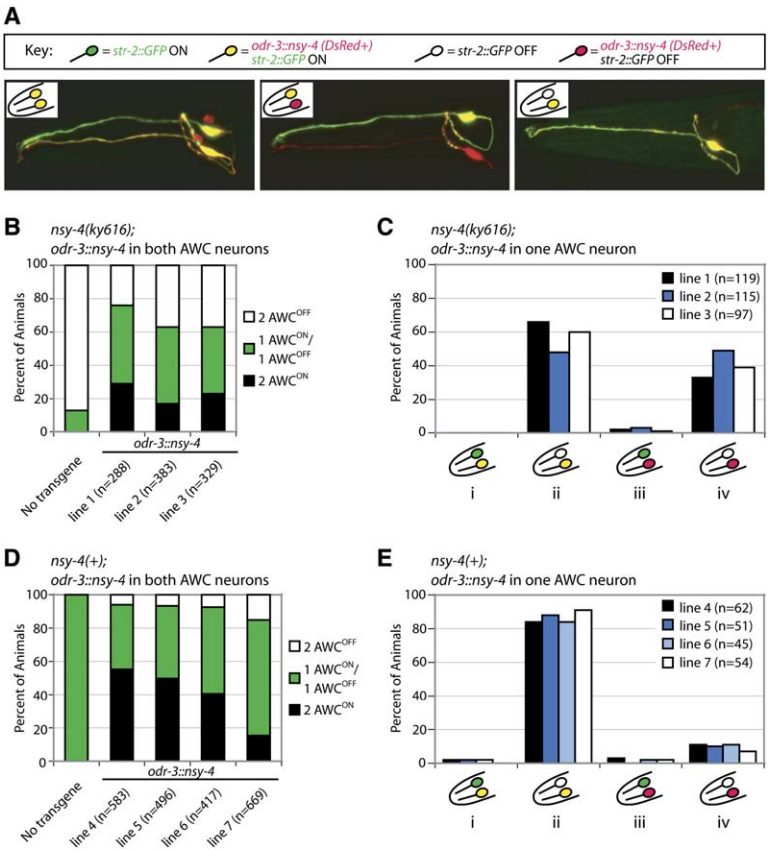

Figure 4. *nsy-4* Mosaic Analysis Reveals Autonomous and Nonautonomous Functions

(A) Wild-type animals expressing an integrated *str-2::GFP* transgene (green) and an unstable transgenic array with both *odr-3::nsy-4* and the AWC marker *odr-1::dsRed* (red). (Left) Array is expressed in both AWCs; *str-2::GFP* is expressed in both AWCs. *odr-1::RFP* is also weakly expressed in both AWB neurons. (Center) Array is expressed in both AWCs; *str-2::GFP* is expressed in 1 AWC. (Right) Mosaic animal. Array is expressed in 1 AWC; *str-2::GFP* is expressed in the same AWC. (B) Rescue of *nsy-4(ky616)* phenotypes in three *Ex[odr-3::nsy-4 odr-1::dsRed]* transgenic lines. The 2 AWC^{OFF} class of transgene-carrying animals is likely due to a combination of incomplete rescue of the *nsy-4* phenotype and *str-2* promoter squelching by *odr-1::dsRed*. (C) Mosaic animals that have lost the array in 1 AWC for strains shown in (B). Diagrams indicate four different classes of mosaic animals, i–iv. (D) *nsy-4(OE)* phenotypes in four *Ex[odr-3::nsy-4 odr-1::dsRed]* transgenic lines in a wild-type background. (E) Mosaic animals that have lost the array in 1 AWC for strains shown in (D). Diagrams indicate four different classes of mosaic animals, i–iv. n, number of animals scored.

was met, but surprisingly, *nsy-4 unc-2* double mutants had a stronger 2 AWC^{ON} phenotype than *unc-2* loss-of-function mutants (Table 1). Like the *unc-36 nsy-4* result, this result suggests that *nsy-4* cannot act solely by inhibiting *unc-2.* In addition, it reveals that *nsy-4* can promote either the AWC^{ON} or the AWC^{OFF} receptor choice, depending on the *unc-2* genotype.

Because it is not clear whether the strongest *nsy-4* allele is null, there are limitations to the interpretations of these double mutants (Han, 2005). However, it is notable that *nsy-4* had straightforward genetic interactions with the downstream kinases but complex genetic interactions with calcium channel subunits. A working model is that NSY-4 (1) antagonizes the function of the UNC-2/UNC-36 calcium channel upstream of CaMKII and (2) has additional functions in AWC that converge on the downstream kinases UNC-43/CaMKII and NSY-1.

NSY-4 Is Required in the Future AWC^{ON} Cell and Affects Lateral Signaling between AWC^{ON} and AWC^{OFF}

Three general models could explain NSY-4 signaling in AWC during receptor choice. First, NSY-4 could provide a permissive, claudin-like adhesion function between AWC neurons that facilitates their signaling. This model appears inconsistent with the 2 AWC^{ON} phenotype of animals overexpressing NSY-4, but modified versions are possible. In the adhesive model, *nsy-4* would be required in both AWC neurons. Second, NSY-4 could act in the future AWC^{OFF} neuron to send a signal to the future AWC^{ON}, perhaps through TARP-like or γ subunit-like modulation of ion channels. Third, NSY-4 could act in the future AWC^{ON} neuron to detect or respond to the signal from AWC^{OFF}. To distinguish among these possibilities, we used genetic mosaic analysis to determine which of the 2 AWC neurons required *nsy-4* activity.

Mosaic analysis was conducted in *nsy-4(ky616);str-2::GFP* animals using unstable extrachromosomal arrays of *odr-3::nsy-4* and the AWC marker *odr-1::dsRed* (Figures 4A and 4B; see Experimental Procedures). Mosaic animals were recognized by loss of dsRed in one of the two AWC neurons, and expression of *str-2::GFP* was scored in the wild-type (dsRed^{+}) and mutant (dsRed^{-}) AWC cell. In one major class of mosaic animals, the cell expressing dsRed became AWC^{ON}, and the mutant cell became AWC^{OFF} (Figure 4C, ii). In the second significant class of mosaic animals, both cells became AWC^{OFF} (Figure 4C, iv). The first class suggests that *nsy-4* acts primarily cell-autonomously in AWC^{ON} to promote AWC^{ON} receptor choice and is consistent with a function in signal reception. The second class can be explained by incomplete rescue from the extrachromosomal arrays (Figures 4B and 4C).

If AWC receptor choice is analogous to the Notch lateral signaling pathway in *Drosophila* and *C. elegans*, feedback from one neuron's decision to become AWC^{ON} could affect receptor choice in the other neuron. Thus, *nsy-4* could participate in lateral signaling that affects both AWC neurons or it could be strictly required in the future AWC^{ON} neuron to execute a decision made by the signaling pathway. Either of these models is consistent with the observed cell-autonomous rescue of *nsy-4*

mutants in AWC^{ON}. To distinguish between these possibilities, we analyzed mosaic animals in lines that overexpressed *odr-3::nsy-4* in a wild-type background [*odr-3::nsy-4(OE)*]. We initially examined three lines in which 41%–55% of the *odr-3::nsy-4(OE)* animals had the gain-of-function 2 AWC^{ON} phenotype (Figures 4D and 4E, transgenic lines 4, 5, and 6). In animals in which only one of the 2 AWC neurons expressed *odr-3::nsy-4*, that neuron became AWC^{ON} significantly more than 50% of the time (Figure 4E, ii). This result supports and confirms the *nsy-4* loss-of-function mosaics by indicating that *nsy-4* overexpression in AWC has a cell-autonomous ability to promote AWC^{ON} receptor choice. Strikingly, the wild-type AWC neuron in these mosaic lines was also affected: instead of becoming AWC^{ON} in 50% of the animals, the wild-type neuron almost always became AWC^{OFF} (Figure 4E, ii). Thus, overexpression of *nsy-4* in 1 AWC neuron had a nonautonomous effect on the other, wild-type AWC neuron. The overexpression effects required an intact *nsy-4* coding region; introducing an early frameshift into the *nsy-4* sequence eliminated both the cell-autonomous and the nonautonomous effect on AWC receptor choice (Figure S4). Based on these results, *nsy-4* is likely to affect signaling between the 2 AWC neurons.

Some stochastic event in normal development makes the 2 AWC neurons different from each other. If *nsy-4* is closely associated with this stochastic asymmetry, even small differences in *nsy-4* expression levels could bias receptor choice. To examine this possibility, we generated mosaic animals in transgenic lines with near-normal levels of *nsy-4* activity. In wild-type animals bearing the array *odr-3::nsy-4* (line 7), only 15% of the animals had a 2 AWC^{ON} gain-of-function phenotype (Figure 4D). When mosaic animals were generated in this strain, the neuron expressing *odr-3::nsy-4* became AWC^{ON} in 90% of the animals, and the wild-type neuron that did not overexpress *odr-3::nsy-4* became AWC^{OFF} (Figure 4E). Thus, even in a nearly wild-type animal, the relative level of *nsy-4* expression in the 2 AWC neurons biased the cooperative decision between alternative receptor choices: the neuron with higher *nsy-4* activity became AWC^{ON} and the neuron with lower *nsy-4* activity became AWC^{OFF}.

Discussion

Following a stochastic but coordinated decision during embryogenesis, the left and right AWC neurons express different odorant receptor genes. NSY-4, a transmembrane protein, acts in AWC to coordinate the alternative AWC^{ON} and AWC^{OFF} receptor choices and is the first molecule to be implicated in lateral signaling between AWC neurons (Figure 5).

The genetic properties of *nsy-4* are consistent with an instructive role in lateral signaling. Reduced *nsy-4* activity results in a 2 AWC^{OFF} phenotype, as expected if the 2 AWC neurons fail to communicate. Overexpression of *nsy-4* causes a 2 AWC^{ON} phenotype, suggesting that *nsy-4* can drive AWC receptor choice. Both transgenic rescue and genetic mosaic analysis indicate that *nsy-4* functions in the AWC^{ON} cell and thus could be part of the receptor system for AWC signaling. In addition, the mosaic analysis of *nsy-4* revealed effects on AWC^{OFF}

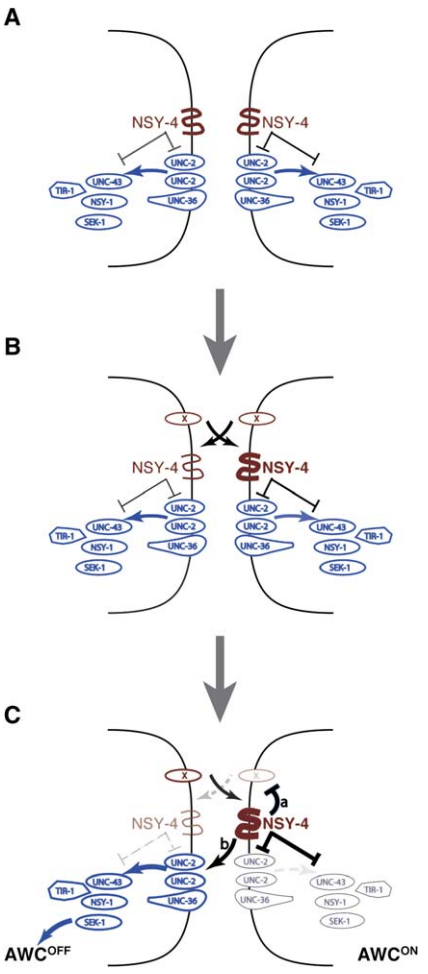

Figure 5. Model for NSY-4 Function in AWC^{ON}/AWC^{OFF} Decision

(A) Early in development, AWC cells are equivalent. Both AWC cells express NSY-4 (red), which promotes the AWC^{ON} receptor choice, and the calcium-MAP kinase cascade (blue), which executes the AWC^{OFF} receptor choice. There may be other genes in the NSY-4 pathway. (B) A signal between AWC cells (X) activates the NSY-4 pathway in both AWC cells. A stochastic event leads to higher activation of the NSY-4 pathway in 1 AWC neuron. (C) Activation of NSY-4 cell-autonomously represses the calcium-MAP kinase cascade, promoting the AWC^{ON} receptor choice. The NSY-4 pathway coordinates lateral signaling by nonautonomously promoting the AWC^{OFF} receptor choice in the contralateral AWC neuron. (a) In one model, NSY-4 could inhibit NSY-4 activation in the contralateral AWC by cell-autonomously suppressing the signal (X). (b) In an alternative model, NSY-4 could stimulate the calcium channel or interacting proteins in the contralateral AWC. Model (b) could explain the paradoxical enhancement of the *unc-2* 2-AWC^{ON} phenotype by an *nsy-4* mutation. Either model is consistent with a claudin-like function of NSY-4 in regulating adhesion.

that implicate *nsy-4* in communication between AWC neurons. *nsy-4::GFP* is expressed transiently in the AWC neurons and fades soon after hatching, an expression pattern consistent with a role in the initial signaling event.

One potential target of *nsy-4* is the calcium channel encoded by *unc-2* and *unc-36.* However, the complex genetic interactions between *nsy-4* and *unc-2* null mutations indicate that *nsy-4* must have other targets in the AWC neurons (Figure 5). These targets, perhaps other channels, converge upon the cell-autonomous

UNC-43/CaMKII-TIR-1-MAP kinase cascade that is active in AWC^{OFF} and inhibited in AWC^{ON} (Chuang and Bargmann, 2005; Tanaka-Hino et al., 2002; Sagasti et al., 2001). Mosaic analysis of *unc-43*, *tir-1*, and *nsy-1* has been conducted in experiments similar to those described here, and all three genes acted mainly cell-autonomously in the AWC^{OFF} cell. These results suggest that the kinases do not have a major role in AWC communication; instead, they execute the AWC^{ON}/AWC^{OFF} decision after it is made. The kinase cascade is required in embryos at the time of synapse formation, a few hours after the AWC axons first extend (Chuang and Bargmann, 2005). UNC-43/CaMKII, TIR-1, and NSY-1/ASK1 are localized to postsynaptic regions of the AWC axon (Chuang and Bargmann, 2005), and a functional NSY-4 protein is present throughout the AWC plasma membrane, so its interaction with these targets could be direct or indirect.

The use of calcium signaling as a mechanism to generate diversity is unusual, but not unprecedented. The neurotransmitter phenotype of spinal cord neurons in *Xenopus* can be respecified by calcium signals (Borodinsky et al., 2004), and the development of fast-twitch and slow-twitch muscle fiber types is also sensitive to calcium signaling through calcineurin (Chin et al., 1998). More speculatively, asymmetric calcium signals have been suggested to play a role in vertebrate left-right body pattern, although the overall pathway is very different from the one used in AWC neurons (Hirokawa et al., 2006).

nsy-4 Acts Autonomously and Nonautonomously in Asymmetric AWC Receptor Choice

The asymmetric receptor choice in AWC^{ON} and AWC^{OFF} is reminiscent of lateral signaling, a process in which developmentally equivalent precursor cells interact with each other to generate distinct cell fates. The key features of lateral signaling are reciprocal communication between cells, a stochastic advantage gained by one cell, amplification of that small difference with feedback, and the execution of mutually exclusive cell fates (Greenwald, 1998; Kimble and Simpson, 1997). The random pattern of asymmetric receptor choice in AWC suggests that cells are equivalent in potential (Figure 5A) but affected by a stochastic event (Figure 5B). The nonautonomous effects of *nsy-4* overexpression suggest the presence of feedback between AWC neurons (Figure 5C).

Lateral signaling is most often mediated by Notch/LIN-12 receptors and DSL family ligands, but Notch homologs appear not to function in the AWC^{ON}/AWC^{OFF} decision (Troemel et al., 1999). Nonetheless, the genetic logic of AWC signaling is similar to the logic of Notch signaling, most notably in the combination of nonautonomous and autonomous functions of *nsy-4*. The *C. elegans* Notch gene *lin-12* has an analogous combination of functions in the AC-VU lateral signaling pathway (Greenwald et al., 1983; Seydoux and Greenwald, 1989). In normal development, either a cell called Z1.ppp or a cell called Z4.aaa can adopt the AC fate, while the other cell becomes a VU cell. This decision is stochastic but coordinated, resulting in one AC and one VU cell in each animal. In *lin-12* loss-of-function mutants, both cells adopt the AC fate (Greenwald et al., 1983). In mosaic animals in which only one cell expresses *lin-12*, coordination between the two cells biases both cells' behavior: the cell with no *lin-12* activity always becomes AC, and the wild-type cell always becomes VU (Seydoux and Greenwald, 1989). Thus, *lin-12* promotes the VU fate cell-autonomously and the AC fate nonautonomously, just as *nsy-4* promotes AWC^{ON} receptor choice autonomously and AWC^{OFF} receptor choice nonautonomously.

nsy-4 and Notch signaling also share an unusual dosage sensitivity that suggests a comparison of their levels between signaling cells. In wild-type animals, even moderate increases in *nsy-4* expression in 1 AWC affect receptor choice in the other, wild-type AWC neuron, which almost always becomes AWC^{OFF}. Similarly, in *Drosophila*, small changes in Notch gene copy number can bias a lateral signaling decision toward the cell with higher levels of Notch (Heitzler and Simpson, 1991). The nonautonomous function of Notch is thought to be accomplished through differential regulation of Notch receptor and DSL ligand activity after activation of Notch (Greenwald et al., 1983; Heitzler et al., 1996; Karp and Greenwald, 2003, 2004; Seydoux and Greenwald, 1989; Wilkinson et al., 1994). The nature of the nonautonomous feedback signal between AWC neurons suggested by these mosaic experiments is unknown.

Notch-independent lateral signaling decisions in other organisms include heterocyst formation in the filamentous cyanobacteria *Anabaena*, which is mediated by the diffusible peptide PatS (Golden and Yoon, 2003), and trichome formation in the plant *Arabidopsis*, which is mediated by direct transfer of transcriptional regulators through plasmodesmata cell junctions (Schiefelbein, 2003). The logic of lateral signaling in metazoa, plants, and prokaryotes may be more general than the molecules that are used to carry out the decision.

A Claudin Superfamily Protein Regulates AWC Receptor Choice

nsy-4 encodes a four-transmembrane domain protein that is related to γ subunits of voltage-activated calcium channels, TARPs/stargazins, and other claudin superfamily members. γ subunits regulate neuronal calcium channels in complex ways that are not fully understood, and TARPs regulate the synaptic localization and activity of AMPA-type glutamate receptors (Arikkath and Campbell, 2003; Heiskala et al., 2001; Kang and Campbell, 2003; Van Itallie and Anderson, 2006). Classical claudin proteins are expressed in epithelial cells and encode components of the apical junction complex (Anderson et al., 2004), a ribbon of adhesion proteins linked to the cytoskeleton. Claudins interact with homotypic or heterotypic claudins in *cis* and in *trans* and recruit or regulate signaling proteins, including cadherins, immunoglobulin proteins, and integrins (Tepass, 2002). Our genetic results suggest that NSY-4 might have both an ion channel regulatory function and a claudin-like receptor/adhesion function.

At a formal genetic level, *nsy-4* antagonizes the calcium channel genes *unc-2* and *unc-36* to promote the AWC^{ON} receptor choice, suggesting that it could act as a regulator of calcium channels. *unc-2* encodes the α1 ion-conducting subunit of the only *C. elegans* N/P/Q-type calcium channel, and *unc-36* encodes a modulatory

α2δ subunit that interacts with *unc-2* and the L-type calcium channel gene *egl-19* (Kerr et al., 2000). In vertebrates, muscle calcium channels require γ subunits to function, but neuronal calcium channels do not require γ subunits, and some are actively inhibited by γ subunits (Arikkath and Campbell, 2003; Kang and Campbell, 2003). For example, overexpression of the γ7 subunit in cultured cells dramatically reduces levels of the coexpressed N-type α1 calcium channel (Moss et al., 2002). A negative regulatory function for *nsy-4* would be consistent with its cell-autonomous function in AWC^{ON} and would tie it closely to the established calcium pathway that regulates AWC receptor choice.

An additional claudin-like function for *nsy-4* is suggested by the morphological defects and reduced viability of *nsy-4(ky627)* and *nsy-4(RNAi)* animals and by the fact that a human claudin could partially rescue AWC receptor choice in *nsy-4* mutants. Claudins are best known for their regulation of differential cell adhesion in epithelia, and *nsy-4* is expressed in subsets of epithelial cells. The claudin-like function should not require calcium channels and therefore might be related to the *unc-2*-independent functions of *nsy-4* in AWC and in other cells. For example, the lethality of *nsy-4(ky627)* is neither shared with *unc-2* and *unc-36*, nor is it suppressed by *unc-36* mutants. By analogy with other claudin superfamily proteins, NSY-4 could regulate other *C. elegans* α1 calcium channel subunits or AMPA-type glutamate receptors, or, like claudins, NSY-4 could have both adhesive functions and signaling functions (Tomita et al., 2001). Stargazin/TARP proteins of the claudin superfamily affect glutamate receptor localization and gating in *cis*, but can also mediate heterotypic claudin-like aggregation of mouse L cells in *trans* (Price et al., 2005). A combination of signaling in *cis* and in *trans* might explain the combination of autonomous and nonautonomous *nsy-4* functions (Figure 5C).

The properties of NSY-4 suggest a link between cell adhesion and ion channel regulation that might be relevant in other contexts in which cell adhesion and channel function are linked, such as the synapse. Although claudins are most highly expressed in epithelia, several are expressed in developing neurons (Kious et al., 2002; Kollmar et al., 2001; Simard et al., 2005; Tomita et al., 2001). It will be interesting to ask whether claudin-related calcium channel regulation, glutamate receptor regulation, and bidirectional adhesion are broadly associated with neuronal differentiation.

Experimental Procedures

Strains

Wild-type strains were *C. elegans* variety Bristol, strain N2. Except for strains containing the *nsy-4::GFP* and *odr-3::nsy-4::GFP* transgenes, all strains contained the integrated *str-2::GFP* transgene *kyIs140 I* (Troemel et al., 1999). Strains were maintained by standard methods (Brenner, 1974).

Mutations and integrated transgenes used in this study included *nsy-4(ky616) IV*, *nsy-4(ky627) IV*, *unc-36(e251) III*, *unc-2(lj1) X*, *unc-2(e55) X*, *unc-43(n1186) IV*, *odr-1(n1933) X*, *kyIs140 I [str-2::GFP*, *lin-15(+)]*, and *kyIs258 X [odr-1::dsRed*, *ofm-1::GFP].* Transgenes maintained as extrachromosomal arrays included seven lines used for mosaic analysis: *kyEx820 (line 1)*, *kyEx819 (line 2)*, *kyEx821 (line 3)*, *kyEx1360 (line 4)*, *kyEx1363 (line 5)*, *kyEx1362 (line 6)*, *kyEx1361 (line 7)* [*odr-3::nsy-4* (50 ng/μl), *odr-1::dsRed*, *ofm-1::GFP*], three lines used for transgenic rescue experiments: *kyEx816 (line 1)*, *kyEx817 (line 2)*, *kyEx822 (line 3)* [*odr-3::nsy-4* (50 ng/μl), *ofm-1::GFP*], and the following additional lines: *kyEx1032* [*nsy-4::GFP*, *ofm-1::dsRed*], *kyEx1042-1048* [*ttx-3::nsy-4*, *ofm-1::GFP*], *kyEx756-758*, *kyEx1050* [*Y38F2AL.1*, *ofm-1::GFP*], *kyEx1051* [*odr-1::dsRed*], *kyEx1057-1062* [*odr-3::nsy-4ΔPDZbm*, *ofm-1::GFP*], *kyEx1056* [*odr-3::nsy-4::GFP*, *ofm-1::dsRed*], *kyEx1064* [*odr-3::nsy-4::GFP*, *str-2::dsRedII*, *ofm-1::RFP*], *kyEx1065-1067* [*nsy-4::GFP*, *odr-3::lin-10::dsRedII*, *ofm-1::dsRed*], *kyEx1068* [*Y38F2AL.1*, *odr-1::dsRed*, *ofm-1::GFP*], *kyEx1391-1393* [*odr-3::claudin-1* (50 ng/μl), *ofm-1::GFP*], *kyEx1396-1400* [*odr-3::hγ7* (50 ng/μl), *ofm-1::GFP*], *kyEx1395*, *kyEx1409-1412* [*odr-3::hγ2* (50 ng/μl), *ofm-1::GFP*], *kyEx1413-1415* [*odr-3::nsy-4 frameshift* (50 ng/μl), *odr-1::dsRed*, *ofm-1::GFP*].

Isolation and Characterization of *nsy-4* Alleles

kyIs140 I (*str-2::GFP*) animals were mutagenized with EMS according to standard protocols (Anderson, 1995,) and F2 animals were subjected to a chemotaxis enrichment for mutants that sensed the AWC^{OFF}-sensed odorant 2,3-pentanedione but failed to sense the AWC^{ON}-sensed odorant butanone. One microliter of butanone (1:1000 dilution in ethanol) was placed on one side of a chemotaxis plate, while 1 μl of 2,3-pentanedione (1:10,000 dilution in ethanol) was placed on the other side; in this choice, most wild-type animals chemotax to butanone. Animals that migrated to butanone were discarded, and the remaining animals were screened for failure to express GFP under a fluorescence dissecting microscope. Additional rounds of the screen were performed without chemotaxis enrichment. The failure to express *str-2::GFP* was confirmed under a compound microscope at 400× magnification.

Chemotaxis assays were performed as described (Bargmann et al., 1993). Odors were diluted in ethanol and tested at standard concentrations (1:1000 butanone, 1:10,000 2,3-pentanedione, 1:200 benzaldehyde).

To examine the initiation and maintenance of *str-2::GFP* expression, gravid adults were allowed to lay eggs for 2.5 hr, the embryos grown for 28.5 hr at 20°C, and late L1s and early L2s assayed for expression of *str-2::GFP* in AWC. DiI staining of amphid neurons in *nsy-4* mutants was performed as previously described (Zallen et al., 1999).

Mapping and Cloning of *nsy-4*

nsy-4(ky616) was mapped on LGIV between single nucleotide polymorphisms in the cosmid C37F5 (nucleotide 13997) and Y38F2AL (nucleotide 63458) using the CB4856 strain (Wicks et al., 2001). A genomic fragment containing only the Y38F2AL.1 reading frame with 7.7 kb of 5′ sequence and 0.9 kb of 3′ sequence was generated by PCR and injected at ~5 ng/μl into wild-type animals. Three transgenic arrays were crossed into *nsy-4(ky616)*, and two rescued the 2 AWC^{OFF} mutant phenotype (defined as >70% of animals scoring as 1 AWC^{ON}/1 AWC^{OFF}). Two additional rescuing lines were generated by injecting DNA directly into *nsy-4(ky616)* mutants. Three rescuing lines were crossed into the *nsy-4(ky627)*, and all rescued the 2 AWC^{OFF} mutant phenotype, the dumpiness, and the poor viability of *nsy-4(ky627)*, indicating that the phenotypes were caused by the same mutation. To identify the *nsy-4* mutations, the *nsy-4* genomic coding regions in *ky616* and *ky627* corresponding to Y38F2AL.1 were amplified by PCR in several pieces, and PCR products were sequenced on both strands.

The *nsy-4(ky627)* lethality, dumpiness, and sterility were rescued by the Y38F2AL.1 genomic fragment, but not by *odr-3::nsy-4* transgenes. Therefore, these phenotypes are probably independent of *nsy-4* function in AWC. Comparable lethal phenotypes were not observed in *unc-2*, *unc-36*, or *unc-43* null mutants, and *unc-36* mutations did not suppress the lethality of *nsy-4(ky627)* (Figure S1). *nsy-4::GFP* fusion genes also cause lethality due to anterior, ventral, or posterior disintegration of the embryo. This lethality suggests that the high-copy transgene interferes with (squelches) expression of the endogenous *nsy-4* gene. The phenotype of *nsy-4(ky627)* and expression of *nsy-4::GFP* suggest an additional role for *nsy-4* in adhesion or signaling between epidermal cells.

Plasmid Construction and Transgenic Strains

Germline transformation was carried out as previously described (Mello et al., 1991). *odr-3::nsy-4*, *odr-3::nsy-4ΔPDZ*, *odr-3::nsy-4::GFP*,

Table 2. Statistical Analysis of Targeted *nsy-4* Expression and Mosaics

Genotype of *odr-3::nsy-4* Transgene Carrying Strain	χ^2 for Independent Behavior of Both Cells		χ^2 for Independent Behavior of Transgene-Expressing Cell		χ^2 for Independent Behavior of Non-Transgene-Expressing Cell	
	χ^2	p	χ^2	p	χ^2	p
nsy-4(ky616); line 1	16	<0.005	8.0	<0.005	4.7	<0.05
nsy-4(ky616); line 2	8.2	<0.05	3.1	NS	2.8	NS
nsy-4(ky616); line 3	26	<0.001	11	<0.001	12	<0.001
wild-type; line 4	62	<0.001	4.3	<0.05	50	<0.001
wild-type; line 5	63	<0.001	8.6	<0.005	47	<0.001
wild-type; line 6	54	<0.001	7.9	<0.01	37	<0.001
wild-type; line 7	126	<0.001	36	<0.001	50	<0.001

nsy-4::GFP, *ttx-3::nsy-4*, *odr-3::nsy-4 frameshift*, *odr-3::hclaudin-1*, *odr-3::hγ7*, and *odr-3::hγ2* were injected at 50 ng/μl, unless otherwise noted. *str-2::dsRedII*, *odr-1::dsRed*, and *odr-3::lin-10::dsRedII* were injected at 30 ng/μl. Lines used for mosaic analysis were coinjected with 7.5 ng/μl of *odr-1::dsRed*. Coinjection markers were 20 ng/μl of *ofm-1::GFP* or *ofm-1::dsRed.*

odr-3::nsy-4

cDNAs were isolated by PCR from a *C. elegans* cDNA library using a primer to the *trans*-spliced leader SL-1 (Krause and Hirsh, 1987) and primers within or near the ORF Y38F2AL.1. Products were cloned into pCR2.1-TOPO and sequenced. Four similar isoforms from these experiments were named "a" through "d." Each isoform was amplified using primers that added a 5′ NheI site and a 3′ KpnI site and subcloned into NheI and KpnI sites of a vector with an EcoRV fragment of the *odr-3* promoter (Roayaie et al., 1998). All four isoforms of *nsy-4* rescued the 2 AWC^{OFF} phenotype of *nsy-4* at similar frequencies when placed behind the *odr-3* promoter (Figure S2).

Clones without the C-terminal PDZ binding motif were generated by amplifying the *nsy-4a* cDNA isoform with a 3′ primer encoding a stop codon instead of the last three amino acids of *nsy-4*. Clones with a frameshift mutation resulting in an early stop codon at position 17 were generated by amplifying the *nsy-4a* cDNA isoform with a 5′ primer inserting a thymidine nucleotide after the second ATG codon at position 29. *ttx-3::nsy-4* was generated by subcloning the *nsy-4a* cDNA isoform into a vector with an ~1.5 kb fragment of the *ttx-3* promoter (Hobert et al., 1997). Clones with human cDNAs (Open Biosystems catalog numbers MHS1768-9143931 [*γ2*], MHS1768-9143931 [*γ7*], and MHS1768-9143840 [*claudin-1*]) behind the *odr-3* promoter were generated by amplifying each cDNA using primers that added a 5′ NheI site and a 3′ KpnI site and subcloning into the *odr-3* promoter vector (Roayaie et al., 1998).

odr-3::nsy-4::GFP

The GFP coding sequence was amplified using primers with 30 bp linkers on each side of GFP, and subcloned into a BsmBI restriction enzyme site between the second and third transmembrane domains of the *nsy-4a* cDNA. The entire fragment was amplified using primers that added a 5′ NheI site and a 3′ KpnI site and subcloned into the *odr-3* promoter vector.

nsy-4::GFP

7.7 kb of the *nsy-4* promoter was subcloned into the *pSM-GFP* vector (a gift from Steve McCarroll). *nsy-4::GFP* fusions caused considerable lethality and malformed heads, tails, and ventral hypodermis in transgenic animals. These phenotypes resembled those of *nsy-4(ky627)* mutants, suggesting that the transgenes interfered with endogenous *nsy-4* function.

Strains containing an extrachromosomal array with both *nsy-4::GFP* and *odr-3::lin-10::dsRedII* were examined for colocalization of dsRedII and GFP in AWC. LIN-10 accumulated in punctate structures in the cell body and the axon (Glodowski et al., 2005; Rongo et al., 1998; Whitfield et al., 1999), while GFP diffused freely. GFP was expressed strongly in the excretory cell processes immediately adjacent to AWC, and as a result the dim AWC expression observed in transgenic lines was unpersuasive. Therefore, mosaic animals were sought in which GFP had been lost from the excretory cell, while dsRedII had been retained in AWC. These animals were then scored for AWC expression of GFP. Three mosaic animals were identified in the L1/L2 stage, and all had GFP expressed in AWC. Seven older mosaic animals generated in the same way lacked detectable GFP expression in AWC.

Genetic Mosaic Analysis

Loss-of-function mosaic analysis was performed on three independent lines with unstable transgenic extrachromosomal arrays [*odr-3::nsy-4, odr-1::dsRed*] in a *nsy-4(ky616)* mutant with a stable integrated *str-2::GFP* transgene. The [*odr-3::nsy-4, odr-1::dsRed*] transgenes did not rescue fully, indicating that they lack sequences required for normal regulation of *nsy-4.* Gain-of-function mosaic analysis was performed on four independent transgenic lines in a wild-type background with a stable integrated *str-2::GFP* transgene. For both loss-of-function and gain-of-function mosaics, loss of the transgene was inferred by loss of the coinjection marker *odr-1::dsRed*, which is expressed strongly in AWC neurons and weakly in AWB neurons. The same strategy using the *odr-3* promoter to drive cDNAs and the *odr-1::dsRed* marker to identify mosaics has previously been used to analyze *unc-43*, *tir-1*, and *nsy-1* in gain-of-function and loss-of-function mosaic analysis experiments (Sagasti et al., 2001; Chuang and Bargmann, 2005). Those three genes were all found to act predominantly cell-autonomously to execute the AWC^{OFF} receptor choice.

str-2 expression data from *nsy-4* mosaic animals were analyzed using the χ^2 test to determine whether the results were consistent with models that predicted (1) random expression of AWC^{ON} and AWC^{OFF} receptor choice, (2) biased expression toward the AWC^{ON} choice, and (3) biased expression toward the AWC^{OFF} choice. For loss-of-function mosaics, all results were consistent with cell-autonomous action in AWC^{ON}, model (2). The low frequency of exceptional animals was consistent with normal variability of transgene expression and the known squelching of *str-2::GFP* by *odr-1::dsRed*. For gain-of-function mosaics, expected values for statistical analysis were generated from internal control animals from the same strain. For example, of the wild-type animals expressing the *odr-3::nsy-4 line 4* transgene in both AWC cells, 55% had a 2 AWC^{ON} phenotype, 39% had a 1 AWC^{ON}/1 AWC^{OFF} phenotype, and 6% had a 2 AWC^{OFF} phenotype. If the AWC cells in mosaic animals were independent, the transgene-expressing cell in mosaic animals should become AWC^{ON} at the same frequency that a cell becomes AWC^{ON} in animals expressing the transgene in both cells, i.e., 74.5%. This corresponds to the 2 AWC^{ON} frequency (55%) and half of the 1 AWC^{ON}/1 AWC^{OFF} frequency (39%). The wild-type, non-transgene-expressing cell was predicted to become AWC^{ON} or AWC^{OFF} at a frequency of 50%. Therefore, the fraction of mosaic animals in which the transgene-expressing cell is AWC^{ON} and the wild-type cell is AWC^{OFF} was predicted to be 37%, animals in which the transgene-expressing cell is AWC^{OFF} and the wild-type cell is AWC^{ON} were predicted at a frequency of 13%, 2 AWC^{ON} animals were predicted at a frequency of 37%, and 2 AWC^{OFF} animals were predicted at a frequency of 13%. Expected and observed numbers of mosaic animals in each class were compared using the χ^2 goodness-of-fit test with 3 degrees of freedom (Table 2).

Wild-type and transgene-expressing cells were then tested individually to determine whether each was affected in mosaic animals, using the χ^2 goodness-of-fit test with 1 degree of freedom (Table 2).

In all gain-of-function lines, both the wild-type and the transgene-expressing cell were affected by the transgene. For *odr-3::nsy-4 line 7*, the transgene-expressing cell was predicted to become AWC^{ON} in 50% of the animals and AWC^{OFF} in 50% of the animals. The observed numbers were 49 AWC^{ON} and 5 AWC^{OFF} neurons in mosaic animals, indicating a significant cell-autonomous bias toward the AWC^{ON} receptor choice ($p < 0.001$). The wild-type cell was expected to become AWC^{ON} in 50% of the animals and AWC^{OFF} in 50% of the animals. In fact, 53 of the wild-type cells became AWC^{OFF} and 1 became AWC^{ON}, indicating a significant bias of the wild-type cell toward the AWC^{OFF} receptor choice ($p < 0.001$, Table 2).

Mosaic analysis was also attempted in animals with a genomic Y38F2AL.1 fragment in *nsy-4(ky616)* and *nsy-4(ky627)* mutant backgrounds. The transgene gave 86%–90% rescue of the 2 AWC^{ON} phenotype without any gain-of-function phenotype, but proved unsuitable for mosaic analysis due to rescue of *nsy-4* even after the *odr-1::dsRed* marker was lost. Similar results were previously observed with *nsy-1* (Sagasti et al., 2001). A likely explanation is that *nsy-4* expression normally begins before the AWC neurons are born, and its function perdures due to earlier expression. This interpretation is consistent with the observed expression of *nsy-4::GFP* early in development, and its expression in cells such as the excretory cell that are closely related to AWC by lineage.

Supplemental Data

The Supplemental Data for this article can be found online at http://www.neuron.org/cgi/content/full/51/3/291/DC1/.

Acknowledgments

We especially thank Kang Shen for his generosity in hosting M.K.V. during part of this work. We thank A. Sagasti, C. Chuang, K. Shen, G. Maro, M. Ding, D. Colón-Ramos, S. Venkatasubrahmanyam, S. McCarroll, M. Gallegos, S. Shaham, M. Hilliard, Y. Zhang, M. Tsunozaki, Y. Saheki, B. Lesch, J. Kennerdell, A. Kahn-Kirby, N. Pokala, and A. Chang for comments, advice, and reagents; Y. Kohara for cDNAs; A. Fire for vectors; and T. Stiernagle of the Caenorhabditis Genetic Center for strains. This work was supported by NIDCD/NIH grant DC004089. M.K.V. was a National Science Foundation predoctoral fellow. C.I.B. is an Investigator of the Howard Hughes Medical Institute.

Received: February 9, 2006
Revised: June 19, 2006
Accepted: June 29, 2006
Published: August 2, 2006

References

Altschul, S.F., Madden, T.L., Schaffer, A.A., Zhang, J., Zhang, Z., Miller, W., and Lipman, D.J. (1997). Gapped BLAST and PSI-BLAST: a new generation of protein database search programs. Nucleic Acids Res. *25*, 3389–3402.

Anderson, P. (1995). Mutagenesis. Methods Cell Biol. *48*, 31–58.

Anderson, J.M., Van Itallie, C.M., and Fanning, A.S. (2004). Setting up a selective barrier at the apical junction complex. Curr. Opin. Cell Biol. *16*, 140–145.

Arikkath, J., and Campbell, K.P. (2003). Auxiliary subunits: essential components of the voltage-gated calcium channel complex. Curr. Opin. Neurobiol. *13*, 298–307.

Bargmann, C.I., Hartwieg, E., and Horvitz, H.R. (1993). Odorant-selective genes and neurons mediate olfaction in *C. elegans*. Cell *74*, 515–527.

Borodinsky, L.N., Root, C.M., Cronin, J.A., Sann, S.B., Gu, X., and Spitzer, N.C. (2004). Activity-dependent homeostatic specification of transmitter expression in embryonic neurons. Nature *429*, 523–530.

Brenner, S. (1974). The genetics of *Caenorhabditis elegans*. Genetics *77*, 71–94.

Chang, S., Johnston, R.J., Jr., and Hobert, O. (2003). A transcriptional regulatory cascade that controls left/right asymmetry in chemosensory neurons of *C. elegans*. Genes Dev. *17*, 2123–2137.

Chang, S., Johnston, R.J., Jr., Frokjaer-Jensen, C., Lockery, S., and Hobert, O. (2004). MicroRNAs act sequentially and asymmetrically to control chemosensory laterality in the nematode. Nature *430*, 785–789.

Chess, A., Simon, I., Cedar, H., and Axel, R. (1994). Allelic inactivation regulates olfactory receptor gene expression. Cell *78*, 823–834.

Chin, E.R., Olson, E.N., Richardson, J.A., Yang, Q., Humphries, C., Shelton, J.M., Wu, H., Zhu, W., Bassel-Duby, R., and Williams, R.S. (1998). A calcineurin-dependent transcriptional pathway controls skeletal muscle fiber type. Genes Dev. *12*, 2499–2509.

Chu, P.J., Robertson, H.M., and Best, P.M. (2001). Calcium channel gamma subunits provide insights into the evolution of this gene family. Gene *280*, 37–48.

Chuang, C.F., and Bargmann, C.I. (2005). A Toll-interleukin 1 repeat protein at the synapse specifies asymmetric odorant receptor expression via ASK1 MAPKKK signaling. Genes Dev. *19*, 270–281.

Duchaine, T.F., Wohlschlegel, J.A., Kennedy, S., Bei, Y., Conte, D., Jr., Pang, K., Brownell, D.R., Harding, S., Mitani, S., Ruvkun, G., et al. (2006). Functional proteomics reveals the biochemical niche of *C. elegans* DCR-1 in multiple small-RNA-mediated pathways. Cell *124*, 343–354.

Glodowski, D.R., Wright, T., Martinowich, K., Chang, H.C., Beach, D., and Rongo, C. (2005). Distinct LIN-10 domains are required for its neuronal function, its epithelial function, and its synaptic localization. Mol. Biol. Cell *16*, 1417–1426.

Golden, J.W., and Yoon, H.S. (2003). Heterocyst development in *Anabaena*. Curr. Opin. Microbiol. *6*, 557–563.

Greenwald, I. (1998). LIN-12/Notch signaling: lessons from worms and flies. Genes Dev. *12*, 1751–1762.

Greenwald, I.S., Sternberg, P.W., and Horvitz, H.R. (1983). The *lin-12* locus specifies cell fates in *Caenorhabditis elegans*. Cell *34*, 435–444.

Han, M. (2005). *C. elegans* Genetics. Genetics (http://www.ergito.com/toc.jsp?bcs=GNTC.2.8) (Virtual Text).

Heiskala, M., Peterson, P.A., and Yang, Y. (2001). The roles of claudin superfamily proteins in paracellular transport. Traffic *2*, 93–98.

Heitzler, P., and Simpson, P. (1991). The choice of cell fate in the epidermis of *Drosophila*. Cell *64*, 1083–1092.

Heitzler, P., Bourouis, M., Ruel, L., Carteret, C., and Simpson, P. (1996). Genes of the Enhancer of split and achaete-scute complexes are required for a regulatory loop between Notch and Delta during lateral signalling in *Drosophila*. Development *122*, 161–171.

Hirokawa, N., Tanaka, Y., Okada, Y., and Takeda, S. (2006). Nodal flow and the generation of left-right asymmetry. Cell *125*, 33–45.

Hobert, O., Mori, I., Yamashita, Y., Honda, H., Ohshima, Y., and Ruvkun, G. (1997). Regulation of interneuron function in the *C. elegans* thermoregulatory pathway by the *ttx-3* LIM homeobox gene. Neuron *19*, 345–357.

Hobert, O., Tessmar, K., and Ruvkun, G. (1999). *The Caenorhabditis elegans lim-6* LIM homeobox gene regulates neurite outgrowth and function of particular GABAergic neurons. Development *126*, 1547–1562.

Johnston, R.J., and Hobert, O. (2003). A microRNA controlling left/right neuronal asymmetry in *Caenorhabditis elegans*. Nature *426*, 845–849.

Johnston, R.J., Jr., and Hobert, O. (2005). A novel *C. elegans* zinc finger transcription factor, *lsy-2*, required for the cell type-specific expression of the *lsy-6* microRNA. Development *132*, 5451–5460.

Johnston, R.J., Jr., Chang, S., Etchberger, J.F., Ortiz, C.O., and Hobert, O. (2005). MicroRNAs acting in a double-negative feedback loop to control a neuronal cell fate decision. Proc. Natl. Acad. Sci. USA *102*, 12449–12454.

Kang, M.G., and Campbell, K.P. (2003). Gamma subunit of voltage-activated calcium channels. J. Biol. Chem. *278*, 21315–21318.

Karp, X., and Greenwald, I. (2003). Post-transcriptional regulation of the E/Daughterless ortholog HLH-2, negative feedback, and birth order bias during the AC/VU decision in *C. elegans*. Genes Dev. *17*, 3100–3111.

Karp, X., and Greenwald, I. (2004). Multiple roles for the E/Daughterless ortholog HLH-2 during *C. elegans* gonadogenesis. Dev. Biol. *272*, 460–469.

Kennedy, S., Wang, D., and Ruvkun, G. (2004). A conserved siRNA-degrading RNase negatively regulates RNA interference in *C. elegans*. Nature *427*, 645–649.

Kerr, R., Lev-Ram, V., Baird, G., Vincent, P., Tsien, R.Y., and Schafer, W.R. (2000). Optical imaging of calcium transients in neurons and pharyngeal muscle of *C. elegans*. Neuron *26*, 583–594.

Kimble, J., and Simpson, P. (1997). The LIN-12/Notch signaling pathway and its regulation. Annu. Rev. Cell Dev. Biol. *13*, 333–361.

Kious, B.M., Baker, C.V., Bronner-Fraser, M., and Knecht, A.K. (2002). Identification and characterization of a calcium channel gamma subunit expressed in differentiating neurons and myoblasts. Dev. Biol. *243*, 249–259.

Koga, M., and Ohshima, Y. (2004). The *C. elegans ceh-36* gene encodes a putative homemodomain transcription factor involved in chemosensory functions of ASE and AWC neurons. J. Mol. Biol. *336*, 579–587.

Kollmar, R., Nakamura, S.K., Kappler, J.A., and Hudspeth, A.J. (2001). Expression and phylogeny of claudins in vertebrate primordia. Proc. Natl. Acad. Sci. USA *98*, 10196–10201.

Krause, M., and Hirsh, D. (1987). A trans-spliced leader sequence on actin mRNA in *C. elegans*. Cell *49*, 753–761.

Lanjuin, A., VanHoven, M.K., Bargmann, C.I., Thompson, J.K., and Sengupta, P. (2003). Otx/otd homeobox genes specify distinct sensory neuron identities in *C. elegans*. Dev. Cell *5*, 621–633.

Lewcock, J.W., and Reed, R.R. (2004). A feedback mechanism regulates monoallelic odorant receptor expression. Proc. Natl. Acad. Sci. USA *101*, 1069–1074.

Maecker, H.T., Todd, S.C., and Levy, S. (1997). The tetraspanin superfamily: molecular facilitators. FASEB J. *11*, 428–442.

Malnic, B., Hirono, J., Sato, T., and Buck, L.B. (1999). Combinatorial receptor codes for odors. Cell *96*, 713–723.

Mathews, E.A., Garcia, E., Santi, C.M., Mullen, G.P., Thacker, C., Moerman, D.G., and Snutch, T.P. (2003). Critical residues of the *Caenorhabditis elegans unc-2* voltage-gated calcium channel that affect behavioral and physiological properties. J. Neurosci. *23*, 6537–6545.

Mello, C.C., Kramer, J.M., Stinchcomb, D., and Ambros, V. (1991). Efficient gene transfer in *C. elegans*: Extrachromosomal maintenance and integration of transforming sequences. EMBO J. *10*, 3959–3970.

Morita, K., Furuse, M., Fujimoto, K., and Tsukita, S. (1999). Claudin multigene family encoding four-transmembrane domain protein components of tight junction strands. Proc. Natl. Acad. Sci. USA *96*, 511–516.

Moss, F.J., Viard, P., Davies, A., Bertaso, F., Page, K.M., Graham, A., Canti, C., Plumpton, M., Plumpton, C., Clare, J.J., and Dolphin, A.C. (2002). The novel product of a five-exon stargazin-related gene abolishes Ca(V)2.2 calcium channel expression. EMBO J. *21*, 1514–1523.

Pierce-Shimomura, J.T., Faumont, S., Gaston, M.R., Pearson, B.J., and Lockery, S.R. (2001). The homeobox gene *lim-6* is required for distinct chemosensory representations in *C. elegans*. Nature *410*, 694–698.

Price, M.G., Davis, C.F., Deng, F., and Burgess, D.L. (2005). The alpha-amino-3-hydroxyl-5-methyl-4-isoxazolepropionate receptor trafficking regulator "stargazin" is related to the claudin family of proteins by Its ability to mediate cell-cell adhesion. J. Biol. Chem. *280*, 19711–19720.

Roayaie, K., Crump, J.G., Sagasti, A., and Bargmann, C.I. (1998). The Gα protein ODR-3 mediates olfactory and nociceptive function and controls cilium morphogenesis in *C. elegans* olfactory neurons. Neuron *20*, 55–67.

Rongo, C., Whitfield, C.W., Rodal, A., Kim, S.K., and Kaplan, J.M. (1998). LIN-10 is a shared component of the polarized protein localization pathways in neurons and epithelia. Cell *94*, 751–760.

Sagasti, A., Hisamoto, N., Hyodo, J., Tanaka-Hino, M., Matsumoto, K., and Bargmann, C.I. (2001). The CaMKII UNC-43 activates the MAPKKK NSY-1 to execute a lateral signaling decision required for asymmetric olfactory neuron fates. Cell *105*, 221–232.

Schafer, W.R., Sanchez, B.M., and Kenyon, C.J. (1996). Genes affecting sensitivity to serotonin in *Caenorhabditis elegans*. Genetics *143*, 1219–1230.

Schiefelbein, J. (2003). Cell-fate specification in the epidermis: a common patterning mechanism in the root and shoot. Curr. Opin. Plant Biol. *6*, 74–78.

Serizawa, S., Ishii, T., Nakatani, H., Tsuboi, A., Nagawa, F., Asano, M., Sudo, K., Sakagami, J., Sakano, H., Ijiri, T., et al. (2000). Mutually exclusive expression of odorant receptor transgenes. Nat. Neurosci. *3*, 687–693.

Serizawa, S., Miyamichi, K., Nakatani, H., Suzuki, M., Saito, M., Yoshihara, Y., and Sakano, H. (2003). Negative feedback regulation ensures the one receptor-one olfactory neuron rule in mouse. Science *302*, 2088–2094.

Seydoux, G., and Greenwald, I. (1989). Cell autonomy of *lin-12* function in a cell fate decision in *C. elegans*. Cell *57*, 1237–1245.

Simard, A., Di Pietro, E., and Ryan, A.K. (2005). Gene expression pattern of Claudin-1 during chick embryogenesis. Gene Expr. Patterns *5*, 553–560.

Simmer, F., Moorman, C., van der Linden, A.M., Kuijk, E., van den Berghe, P.V., Kamath, R.S., Fraser, A.G., Ahringer, J., and Plasterk, R.H. (2003). Genome-wide RNAi of *C. elegans* using the hypersensitive *rrf-3* strain reveals novel gene functions. PLoS Biol. *1*, E12.

Tanaka-Hino, M., Sagasti, A., Hisamoto, N., Kawasaki, M., Nakano, S., Ninomiya-Tsuji, J., Bargmann, C.I., and Matsumoto, K. (2002). SEK-1 MAPKK mediates Ca2+ signaling to determine neuronal asymmetric development in *Caenorhabditis elegans*. EMBO Rep. *3*, 56–62.

Tepass, U. (2002). Adherens junctions: new insight into assembly, modulation and function. Bioessays *24*, 690–695.

Tomita, S., Nicoll, R.A., and Bredt, D.S. (2001). PDZ protein interactions regulating glutamate receptor function and plasticity. J. Cell Biol. *153*, F19–F24.

Troemel, E.R., Sagasti, A., and Bargmann, C.I. (1999). Lateral signaling mediated by axon contact and calcium entry regulates asymmetric odorant receptor expression in *C. elegans*. Cell *99*, 387–398.

Van Itallie, C.M., and Anderson, J.M. (2006). Claudins and epithelial paracellular transport. Annu. Rev. Physiol. *68*, 403–429.

Wes, P.D., and Bargmann, C.I. (2001). *C. elegans* odour discrimination requires asymmetric diversity in olfactory neurons. Nature *410*, 698–701.

White, J.G., Southgate, E., Thomson, J.N., and Brenner, S. (1986). The structure of the nervous system of the nematode *Caenorhabditis elegans*. Philos. Trans. R Soc. Lond. B Biol. Sci. *314*, 1–340.

Whitfield, C.W., Benard, C., Barnes, T., Hekimi, S., and Kim, S.K. (1999). Basolateral localization of the *Caenorhabditis elegans* epidermal growth factor receptor in epithelial cells by the PDZ protein LIN-10. Mol. Biol. Cell *10*, 2087–2100.

Wicks, S.R., Yeh, R.T., Gish, W.R., Waterson, R.H., and Plasterk, R.H. (2001). Rapid gene mapping in *Caenorhabditis elegans* using a high density polymorphism map. Nat. Genet. *28*, 160–164.

Wilkinson, H., Fitzgerald, K., and Greenwald, I. (1994). Reciprocal changes in expression of the receptor *lin-12* and its ligand *lag-2* prior to commitment in a *C. elegans* cell fate decision. Cell *79*, 1187–1198.

Yu, S., Avery, L., Baude, E., and Garbers, D.L. (1997). Guanylyl cyclase expression in specific sensory neurons: a new family of chemosensory receptors. Proc. Natl. Acad. Sci. USA *94*, 3384–3387.

Zallen, J.A., Kirch, S.A., and Bargmann, C.I. (1999). Genes required for axon pathfinding and extension in the *C. elegans* nerve ring. Development *126*, 3679–3692.